Evaluating and Predicting Changes Occurring on the Coastlines of Jeddah City Using Satellite Images

Hamdy A. Aboulela[1,2] · Rashad A. Bantan[1] · Ramadan A. Zeineldin[3,4]

Abstract
The current study highlights the usefulness of satellite images in monitoring and predicting changes occurring on shorelines through a bi-dimensional strategy—data based and situational based. Three coastal areas of Jeddah city were selected as the study areas: Salman Bay, Sharm Abhar and Jeddah Port. For the data-based dimension, data collected through satellite images were used in the analysis covering the period from 1972 to 2016. Four regression models were used to study the variation in the coastal borders of the study area. Predictions for the next 9 years, i.e., up to 2025, were carried out using the four regression models. The results revealed that an area reduction has been witnessed in all the areas under study. Another fact that came to the limelight is the proximity of the objective results with the expectations of experts, thus providing credence to the appropriateness of employed statistical models. For situational-based dimension effects, various anthropogenic activities and geo-environmental natural processes in the study area were identified. Based on the findings of the study, continuous monitoring of the coastal areas is suggested along with maintaining a concrete database. The proposed techniques can be extended to study coastal reduction and extension in other regions as well.

Keywords Shoreline · Prediction · Anthropogenic · Geo-environmental

1 Introduction

Monitoring and predicting changes on coastlines are significant predictors to support improvement and safety of the environment. Coastlines are unique and significant linear landscapes with active environments [1], demarcating the line of interaction between terrestrial and marine environments. [2] Satellite images present significant changes in the coastline of the region. The western coastal zone margins of Saudi Arabia, i.e., the Red Sea, have experienced land use changes due to anthropogenic activities and the development of ongoing mitigation plans [3]. Additionally, the zone is also subjugated by geo-environmental influences such as coastline changes, sediment dynamics, erosion and accretional processes, saltwater intrusion and irrational land use. The coastal borders of Jeddah city along the Red Sea and adjacent surroundings represent a perfect example of an affected coastal border profile. More studies are warranted along the coastlines to establish a scientific database of the changes occurring at the coastlines of Jeddah city and its surroundings. Furthermore, understanding the processes affecting changes in coastlines and quantifying the rate of coastline changes are crucial for better coastal area management [4]. Therefore, the prediction statistical techniques for the future analysis of rates of coastline changes of the study area are suitable tools for recognizing temporal and spatial trends of beach erosion and accretion activated by natural processes and various anthropogenic activities. The study area reflects a unique preemptive dynamic region in Saudi Arabia. It has a variety of human activities due to its proximity to the city of Makkah. Moreover, the geographic location on the coast of the Red Sea makes the city of Jeddah one of the most significant marketable towns in Saudi Arabia. The study area has a multiplicity of recreational activities alongside the coastline of the Jeddah governorate. In addition, it is one of the vital issues for attracting tourists, which qualify it for

✉ Hamdy A. Aboulela
  aboulel1_004@yahoo.co.uk

1 Faculty of Marine Sciences, King Abdul Aziz University, Jeddah, Kingdom of Saudi Arabia

2 Faculty of Science, Suez Canal University, Ismailia 41522, Egypt

3 Deanship of Scientific Research, King Abdul Aziz University, Jeddah, Kingdom of Saudi Arabia
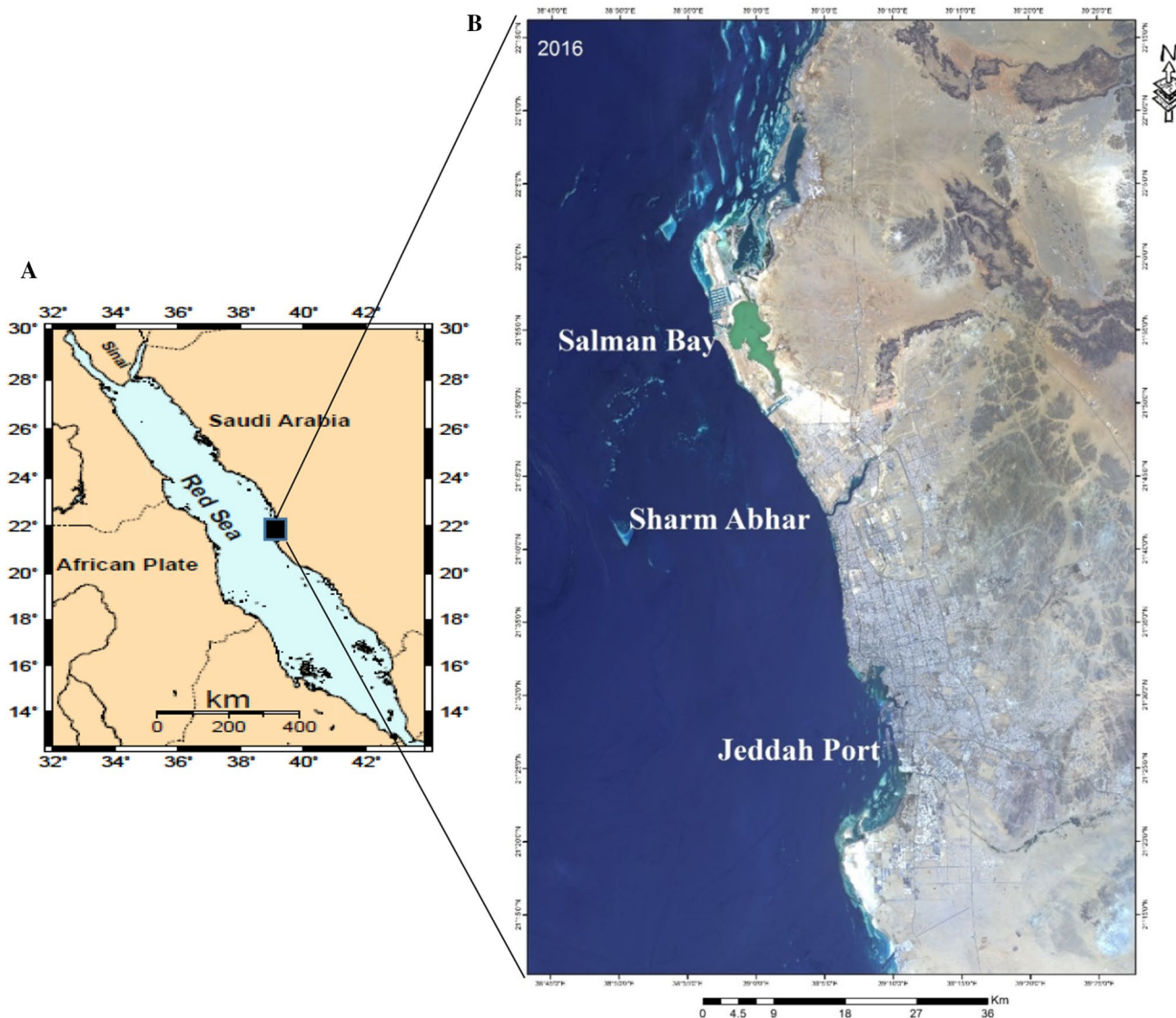
4 ISSR, Cairo University, Giza, Egypt

Fig. 1 **a** Location map displaying the study area and its surroundings. **b** Spatial border of the study area displayed on satellite image 2016. *Source*: National Authority for Remote Sensing and Space Sciences (NARSS)

the comprehensive concept of touristic sustainable development. In general, investment developments and misuse of the land lead to the decrease in the recreational areas along the coastline and depletion of marine natural resources. The present study aims to delineate the rate of change of the coastline changes in the study area from satellite images from 1972 to 2016. In addition to the generation of a database of the changes occurring in the study area, sustainable management is envisaged. An analysis of the local changes that have occurred on the coastlines of Jeddah and its surrounding areas due to the effects of geo-environmental natural processes and various anthropogenic activities is performed. Predictions of variations in coastal border changes constitute an important area for research because there are rapid changes in coastal borders all

over the world. Statistical prediction techniques such as linear regression and nonlinear regression models such as logarithmic models, inverse models, power models and polynomial models are used to predict variations in future border changes. Other methods are used to evaluate the performance of statistical prediction techniques such as the mean square error and mean absolute deviation. In addition, simulation approaches are used in predictions of future changes, and in this paper, simulation found better predictions for Jeddah Port variation changes.

Table 1 Materials and documentation used in the current study

| Materials and documents	Description			
	Spacecraft id/sensor	Acquired date	Path/raw	Pixel resolution (m)
Landsat	Landsat_1/MSS	1972-09-29	170/45	60
Satellite images	Landsat_5/TM	1984-06-06	170/45	30
Source:	Landsat_5/TM	1990-09-11	170/45	30
National Authority for Remote Sensing and Space Sciences	Landsat_7/ETM	2000-02-03	170/45	30
	Landsat_8/OLI_TIRS	2016-06-14	170/45	30
Geologic maps	Scale 1:250,000 [7]			
Topographic maps	Contour interval 20 m. Digital elevation model (DEM), resolution 30m2			
Software	ENVI 5.3 for image processing (ENVI image analysis software) ArcGIS 10.3 for GIS applications			
A statistical techniques	Linear regression, Logarithmic, inverse and power techniques Mean square error and mean absolute deviation methods.			
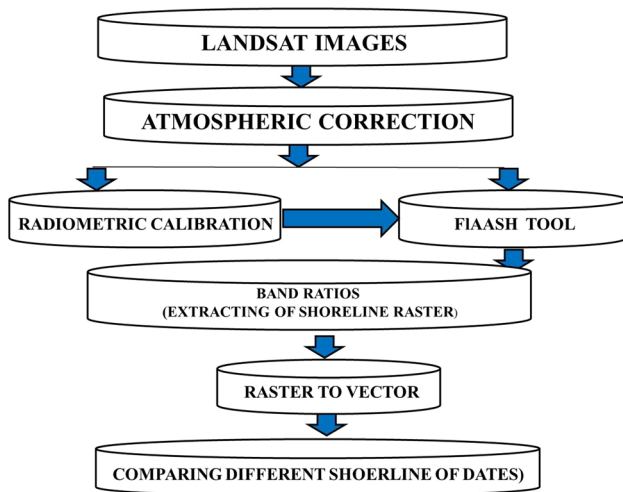
Fig. 2 Flow diagram of the procedural steps of the developed techniques

Table 2 Changes in the spatially bordered area for the Salman Bay area, Sharm Abhar and Jeddah Port during 1972–2016 from classified images

Year	Change of spatial bordered area in km^2		
	Salman Bay (Area in km^2)	Sharm Abhar (Area in km^2)	Jeddah Port (Area in km^2)
1972	25.97	6.42	58.98
1984	42.64	5.93	42.25
1990	23.89	5.35	43.86
2000	30.99	4.59	41.87
2016	30.66	5.18	42.20

2 The Study Area

The present study area lies in the middle of the eastern coastal margin of the Red Sea and to the west of Saudi Arabia (Fig. 1a) at latitude 20°:50′:57″–22°:18′:35″ and longitude 38°:55′:42″–39°:25′12″(Fig. 1b). It occupies areas bordered by Salman Bay, Sharm Abhar and Jeddah Port from the northern to the southern parts of the city. The city of Jeddah, which is situated lengthwise on the shoreline plain, is approximately 10 km wide and restricted to the east by a number of highland chains with an altitude of approximately 200 m [5], [6]. There are a number of valleys in the hilly region of the city, which spread the slopes into the coastal plain regions, the coastal borders of Jeddah and its surroundings [7]. The area under study constitutes a slice of the western Arabian Shield, which is completely covered by Neoproterozoic rocks comprising different types of volcaniclastics, with some changeability of intrusive plutonic igneous rocks. Most of these rocks are shielded by Tertiary and Quaternary lavas and sediments and in seats by recent sediments and sabkhas along the coastlines of the study area [7].

3 Materials and Methods

In general, remote sensing and geographic information system techniques reflect prevailing and actual tools and are extensively employed for identifying the spatiotemporal dynamics of coastline changes. In the present study, satellite images for the period between 1972 and 2016 were obtained from Landsat, MSS, TM, ETM+ and Landsat_8_images. The data from these images were processed; the data were

analyzed and integrated with data from geological maps [7], field surveys and other ancillary data. Additionally, statistical techniques such as linear regression, logarithmic, inverse and power techniques are used to predict the future rate of coastline changes of the three areas in the study area, Salman Bay, Sharm Abhar and Jeddah Port, to 2025. The change in coastal border areas is due to the variations of different anthropogenic activities such as industrial development, unsystematic projects such as the establishment of tourist villages and resorts and filling work. Additionally, the simulation approach is used in the prediction process for the three areas. The results of the prediction are compared with the actual data and evaluated using the mean square error and mean absolute deviation methods. Table 1 shows all the materials and documentation used in the present study.

3.1 Methodology and Data Processing

Numerous methods for coastline extraction from satellite images have been applied. Figure 2 shows a flow diagram of the procedural techniques utilized during the present study. Four main stages were used to analyze the numerical data (Table 2) in this study. Four procedures were applied in a time sequence manner.

3.2 Atmospheric Correction

In general, satellite images are affected by atmospheric particles from engagement and scattering of radiation from the Earth's surface. To retrieve surface reflectance, atmospheric corrections were made. The surface reflectance phenomenon is defined as the surface categories extracted from remotely sensed imagery. The atmospheric corrections were made to enhance the image accuracy when they are classified. During atmospheric corrections, radioactive transfer algorithms considering atmospheric optical properties are used and adjusted. Overturning ways that derive the surface reflectance of images were used. The ENVI 5.3 image analysis software involved two steps, i.e., radiometric calibration and surface reflection employing the FLAASH module, which was used for image atmospheric correction.

3.3 Radiometric Calibration

Radiometric calibration refers to the ability to convert digital numbers recorded by satellite imaging systems into physical units. Those units are either radiance (W/m^2/sr/ µm) or apparent top-of-atmosphere reflectance. Vicarious-based Absolute Top-of-atmosphere reflectance is 0 to 1.0. This option is available if the image gains, offsets, solar irradiance, sun elevation and acquisition time are defined in metadata. The ENVI 5.3 image analysis software tool provides such values from metadata analysis of images,

which are then used to compute reflectance employing the following equation

$$\rho_\lambda = \frac{\pi L_\lambda d^2}{\text{ESUN}_\lambda \sin \theta} \qquad (1)$$

where L_λ = radiance in units of W/(m^2 * sr * µm); d = earth–sun distance in astronomical units; ESUN$_\lambda$ = solar irradiance in units of W/(m^2 * µm); θ = sun elevation in degrees

3.4 Fast Line-of-Sight Atmospheric Analysis of Hypercubes (FLAASH)

FLAASH is a modified tool derived from MODTRAN, which according to [8, 9] could solve errors in previous tools. FLAASH depends on image metadata and modeling standard column water vapor. During the current study, atmospheric and tropospheric models were applied; the tropical model is an aerosol model that uses images positioned on the troposphere, whereas the tropospheric model is applied under calm and clear (visibility greater than 40 km) conditions over the land and consists of small-particle components of the rural model. FLAASH starts from the standard equation of spectral radiance at a sensor pixel 'L' that applies to the solar wavelength range (thermal emission is neglected) and flat Lambertian materials or their equivalents. The equation is as follows:

$$L = \left(\frac{A\rho}{1 - \rho_e S} \right) + \left(\frac{B\rho_e}{1 - \rho_e S} \right) + L_a$$

where ρ is the pixel surface reflectance; ρ_e is an average surface reflectance of the pixel and a surrounding region; S is the spherical albedo of the atmosphere; L_a is the radiance backscattered by the atmosphere; and 'A' and 'B' are coefficients that depend on atmospheric and geometric conditions but not on the surface.

3.5 Shoreline Positions and Detecting

Extracted data from Landsat images were used to compare the shoreline positions covering the period from 1972 to 2016. Landsat images from different dates covering the period from 1972 to 2016 were used to detect shoreline changes during the study period. Depending on the band ratio, which reduces environmental influences on the digital number (DN) value assigned to a pixel in a digital image, the DN values of a single band [10] are determined by utilizing the green, near-infrared (NIR) and shortwave infrared (SWIR) 1 bands. The green band is sensitive to water turbidity, which aids in differentiating vegetation classes. The near-infrared band (NIR), absorbed in water, becomes useful

in extracting water bodies and differentiating between dry and moist soils. The SWIR1 band displays a high contrast between land and water classes and discriminates moisture contents in soil and vegetation [11]. Other studies have used the NIR band [12], whereas we have selected both the green (NIR) and shortwave (SWIR1) bands, achieving significantly suitable main results, particularly during the analysis of images from 1984.

(a) NDWI: Normalized Difference Water index with band ratios of three bands (green, NIR and SWIR1 bands) by using the ENVI program. Simply: (band green/NIR*band green/SWIR1) by using the band ratio image and adding to the NDWI index.

After classification, shoreline classes were converted to vector line for five images acquired on different dates.

3.6 Statistical Techniques

In the current study, regression methods and the simulation approach are used to predict the future of the study area, especially along the three areas of Salman Bay, Sharm Abhar and Jeddah Port from 1972 to 2025. Four regression methods have been selected. These methods are used for the three above-mentioned areas. Since the area of Jeddah Port will be expanded in the future, it was deemed pointless to apply the regression methods to this area. We used a simulation approach to predict the future area for Jeddah Port. In addition, a simulation method was used for the other two areas. In this section, the regression methods and simulation approach are briefly presented

3.6.1 Regression Models

Regression methods are used extensively for prediction. Multiple linear regression techniques are used to estimate
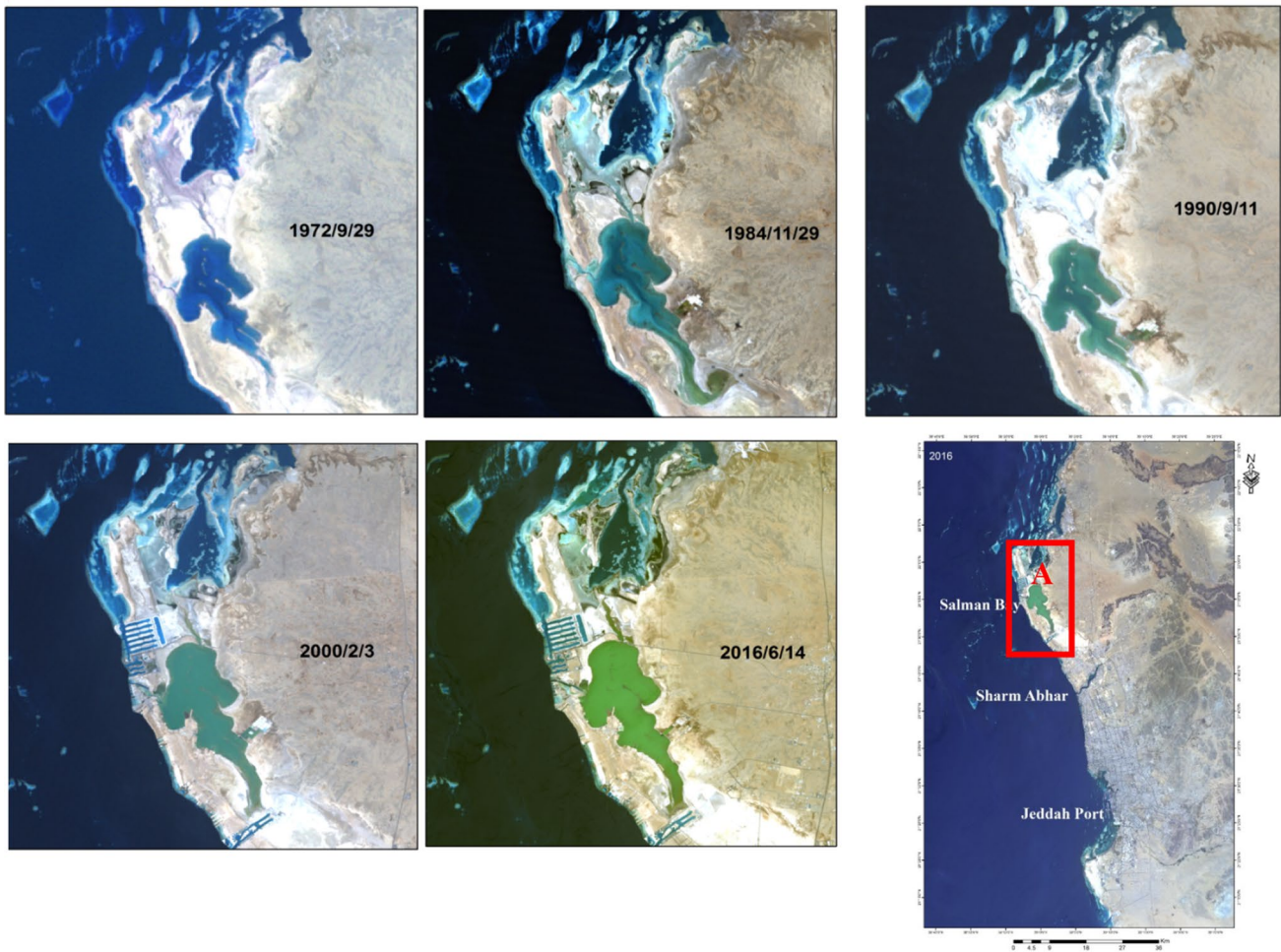

Fig. 3 Exposure of the coast to extensive filling processes, showing destruction of coastal features in the area of Salman Bay. (A) Location map display of Salman Bay
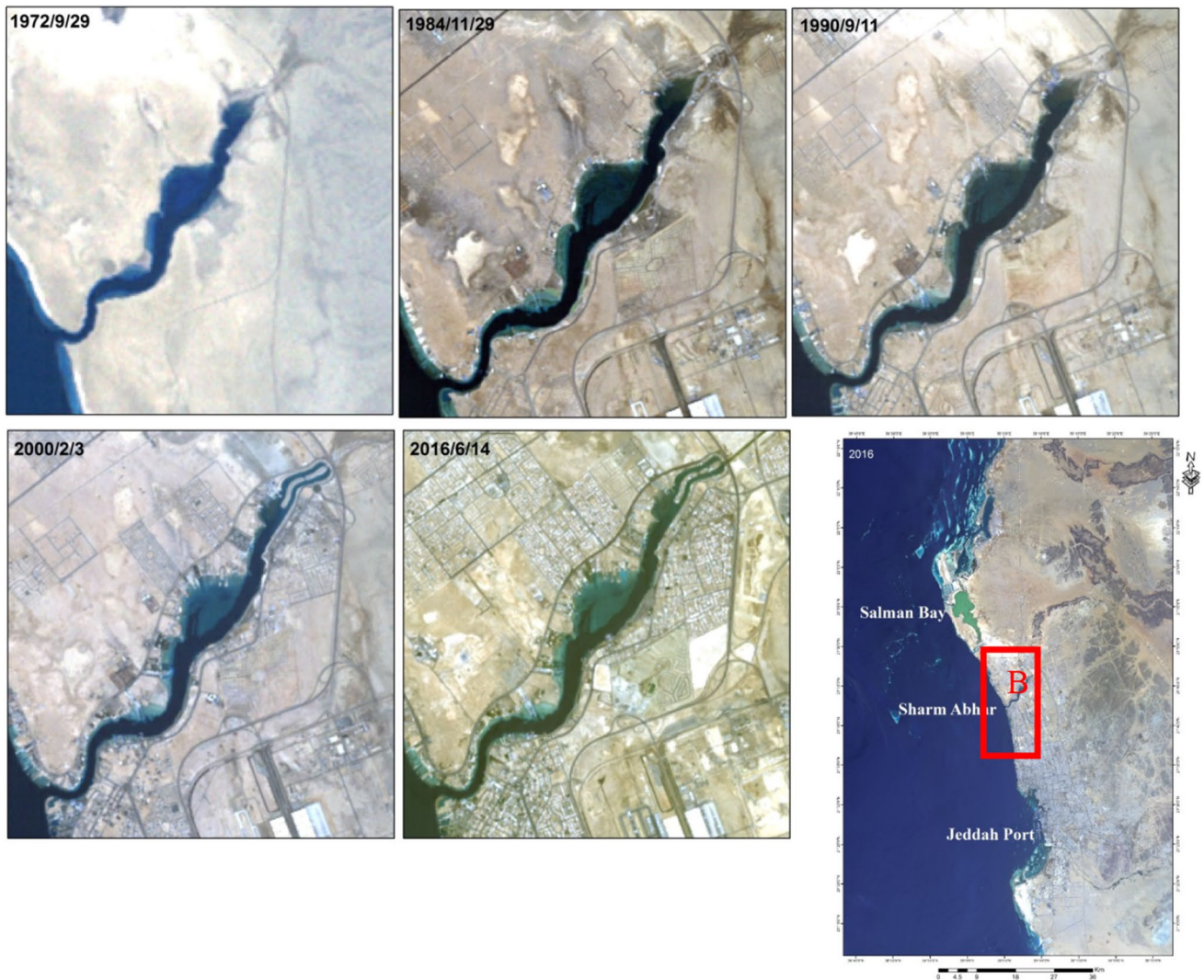
Fig. 4 Anthropogenic activities leading to severe environmental degradation of the marine environment in the Sharm Abhar area. (B) Location map display of the Sharm Abhar area

the shoreline change rate for the location of partial discharge pulse along the windings [13]. As there are different regression models, curve estimation is performed, and the suitable models with the highest R^2 are selected. The models used are a linear regression model, logarithmic regression model, inverse regression model and power regression model. Their equations are as follows:

Linear model: $Y = b0 + (b1 \times t)$
Logarithmic model: $Y = b0 + (b1 \times \text{Ln}(t))$
Inverse model: $Y = b0 + (b1 \times 1/t)$
Power model: $Y = b0 \times tb1)$

For all the forecasting models, the error is estimated. Two methods are used to measure the forecasting error. The mean

absolute deviation (MAD) and mean squared error (MSE) are used according to [14, 15].

The mean absolute deviation: $\text{MAD} = 1n\ t = \text{Ln}\ |Yt–Yt|$
The mean squared error: $\text{MSE} = \text{Ln}\ (Yt–Yt)^2$

3.6.2 Simulation

Simulations are used extensively in predictions in all fields, such as predictions of sinter yield and strength for the iron ore sintering process [16]. Many studies have been carried out to predict CO_2 sorption isotherms and the CO_2-induced plasticization behaviors of glassy polyimides [17]. Another example is the simulation of occupants' evacuation behaviors and casualty predictions in buildings during earthquakes in China [18]. Additionally, simulation is used to predict
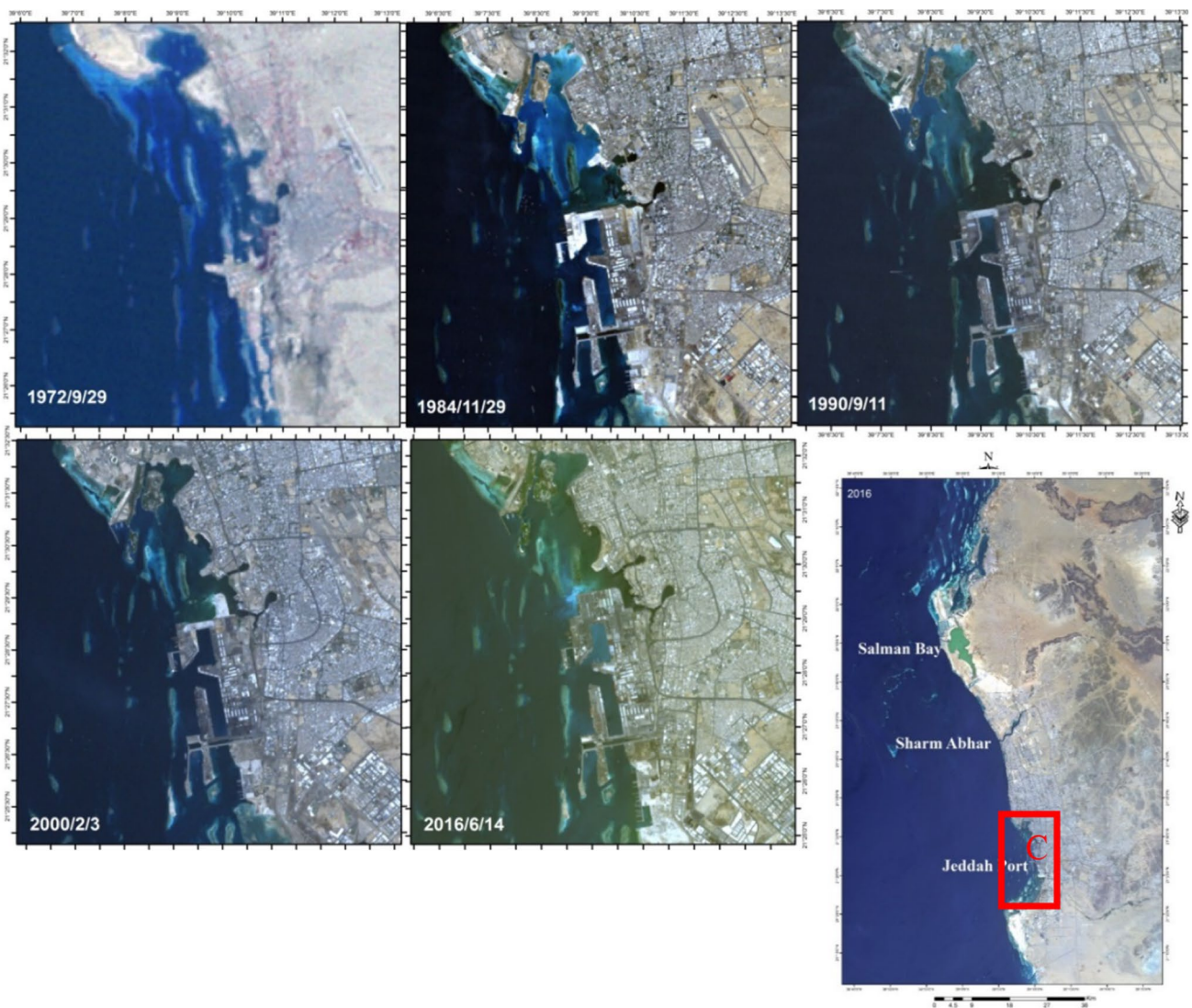
Fig. 5 Changes in the coastline shape due to dredging operations and disposition of marine debris at Jeddah Port. (C) Location map display of the Jeddah Port

the cooling condition and microstructure in friction hydro pillar processing [19]. Simulation is used in GIS in many ways, for example, [20] used a simulation to calculate the maximum intensity of urban heat islands. [21] developed a GIS-based simulation to select biofuel facility locations. [22] developed a GIS-based simulation to obtain the annual optimal placement and size of photovoltaic (PV) units for the next 2 decades in a campus area environment. [23] used a simulation approach for coastal changes at both geological and engineering time scales. Other different applications for simulations with GIS are presented in recent research. In this study, the simulation approach is used to predict the future areas for the three bays. The applied steps are as follows:

(a) The actual data were fitted to the available fitting distributions in input analyzer.
(b) The distributions with the least square error were selected.
(c) Areas for years 1972–2025 are generated using these best fit distributions.
(d) The mean square error and mean absolute deviation for each of the predicted values were calculated.
(e) The best distribution(s) were selected.

For example, when simulation is applied to study the variation in the coastal borders for Jeddah Port, actual data are fitted to ten statistical distributions using the Arena input analyzer. The Arena package provides the square error and the equation that will be used in predictions for all the fitted
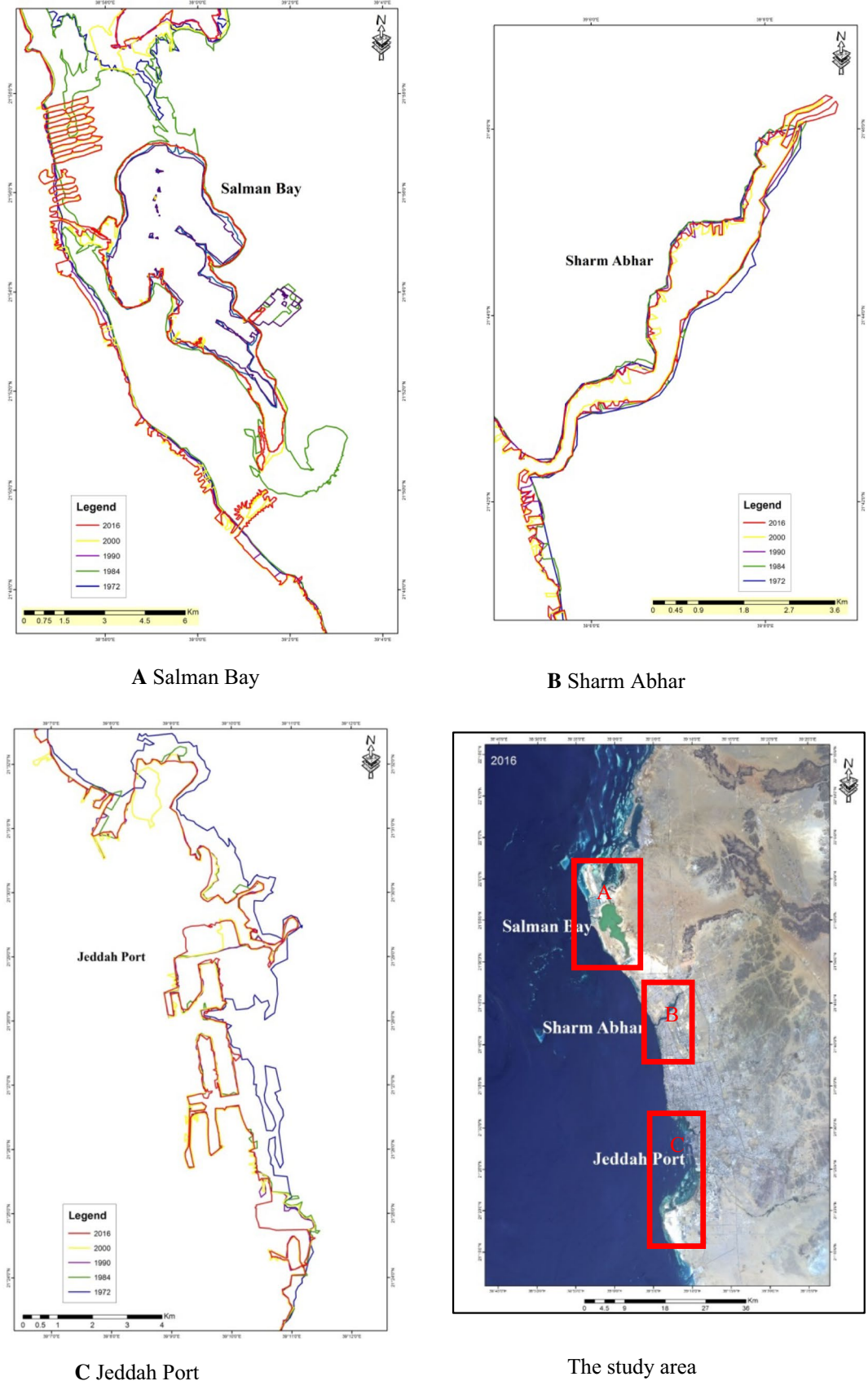
A Salman Bay

B Sharm Abhar

C Jeddah Port

The study area

Fig. 6 Comparison of changes spatially bordered by the (A) Salman Bay area; (B) Sharm Abhar area; and (C) Jeddah Port

distributions, and the distribution with the least square error is selected. For Jeddah Port, the Arena input analyzer provided the following statistical distributions with their square errors: beta, Lognormal, Weibull, gamma, Erlang and exponential; the following square errors are in the sequence 0.059242, 0.097205, 0.129309, 0.167684, 0.184863 and 0.184863. The best fitting distribution is the beta distribution because it has the smallest square error. After that, the equation provided by the Arena input analyzer is used to predict future variations in the coastal borders for Jeddah Port. The distributions' equations with minimum square errors are applied and compared, with involvement by the decision maker in selecting the more suitable distribution.

4 Results and Discussion

In general, image processing is used to assist with visual interpretation and can highlight specific image information, i.e., by maximizing the distinction between light and dark ratios of an image or emphasizing a specific data variety or spatial area (e.g., water vs. land) in an image. The output data were saved as a vector file, enabling the analysis of changes to coastal borders by using ArcGIS 10.3 in a geographic information System (GIS) software application. The changes in coastal border areas during the period 1972–2016 were extracted from images by using measurement tools of ENVI 5.3 image analysis software. The study showed changes to the shoreline due to geo-environmental natural processes and anthropogenic activities. Figure 3 displays the exposure of the coast to extensive unplanned projects and filling processes leading to the destruction of coastal features of Salman Bay. The anthropogenic activities have led to severe environmental degradation of the marine environment of the Sharm Abhar area, as shown in Fig. 4. Figure 5 shows the changes in the shape of the coastline, especially those due to the direct impact of dredging operations and the marine debris left on the coastal borders of Jeddah Port. To monitor and predict changes in coastal borders, it is essential to compare changes to coastal borders with extracted coastlines from reliable and accurate maps. To monitor and predict changes, an image-driven reference dataset was utilized [24]. The accurate image was provided by fusing Landsat /ETM + multispectral bands with Landsat /ETM + panchromatic bands. The changes to coastal borders from true images are extracted via visual interpretation. Figure 6 shows the changes in the images of the study area for the coastlines of Salman Bay (Fig. 6A), Sharm Abhar (Fig. 6B) and Jeddah Port (Fig. 6C) in the years 1972, 1984, 1990, 2000, and 2016. When changes occurring in the areas of Salman Bay (Fig. 6A), Sharm Abhar (Fig. 6B) and Jeddah Port (Fig. 6C) are compared, it was found that

natural processes and anthropogenic activities during the period from 1972 to 2016 were responsible for the changes (Table 2). There were significant changes in the coastal borderline area of 30.66 km^2 in 2016 compared to that of 25.97 km^2 recorded in 1972, especially in the Salman Bay area. The changes revealed that the area of this part had increased to approximately 4.69 km^2 from 1972 to 2016. These changes in Salman Bay area are attributed to the initialization of random projects and filling work (Table 2). The coastal borderline area of Sharm Abhar in 1972 was 6.42 km^2 compared to 5.18 km^2 in 2016, revealing a decrease in area of 1.24 km^2 from 1972 to 2016. These changes are also attributed to anthropogenic activities such as dredging operations (Table 2). In the case of Jeddah Port, the area of 58.98 km^2 in 1972 was found to have decreased to 42.20 km^2 in 2016, a reduction of 16.78 km^2 from 1972 to 2016. These changes are also attributed to anthropogenic activities, such as the establishment of random projects and filling work (Table 2). Applying
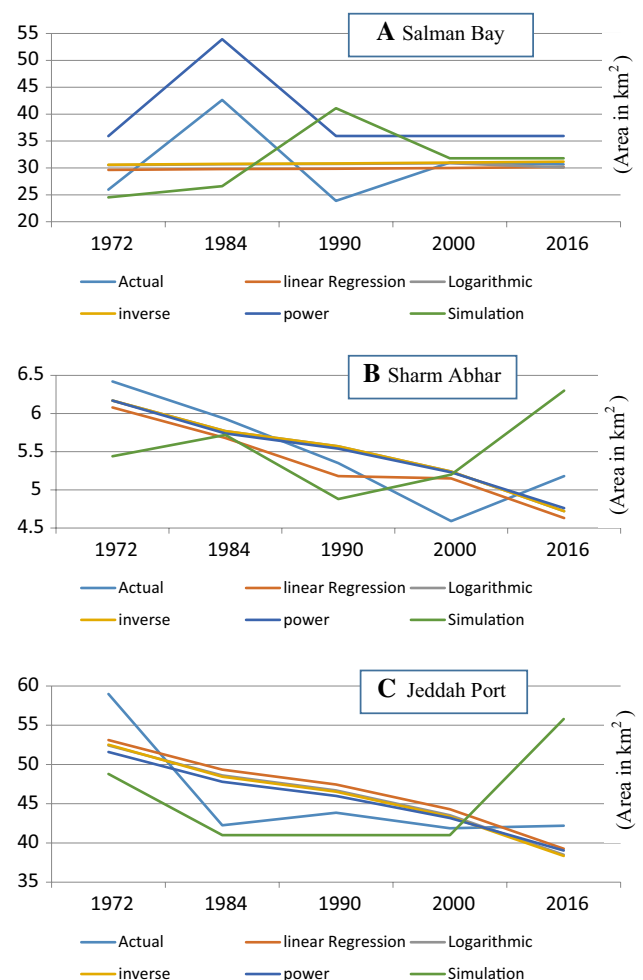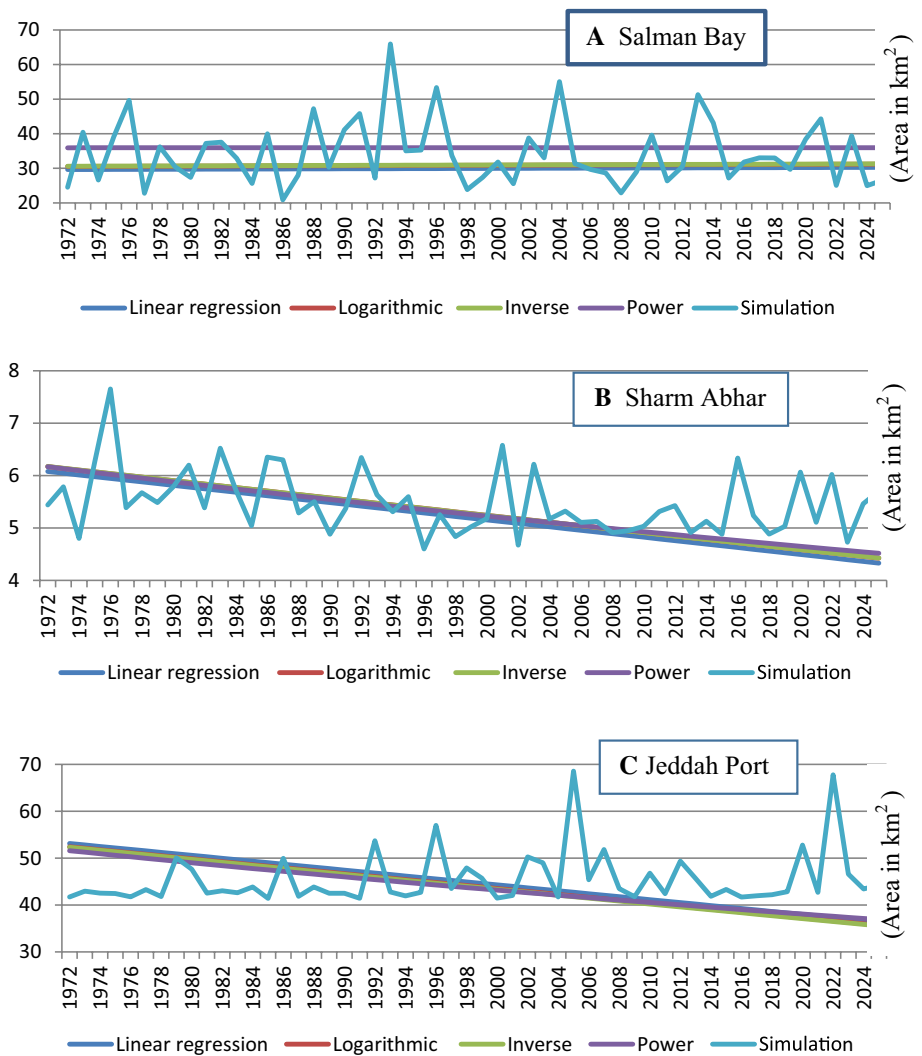

Fig. 7 The actual data compared with the predicted data for **a** Salman Bay, **b** Sharm Abhar and **c** Jeddah Port

Fig. 8 The results of prediction methods for **a** Salman Bay, **b** Sharm Abhar and **c** Jeddah Port

statistical techniques, the results produced from the prediction methods are compared with the actual data; the MSE and mean absolute deviation (MAD) are calculated to compare the results of the methods. IBM SPSS 25 package is used for prediction for the three areas depending on the collected real data. Curve estimation is performed to select the methods with the highest determination factor (R^2). Arena simulation package version: 14.70.00 is used to develop simulation models. The models with the least square error are selected.

4.1 Comparison of the Predicted and Actual Values

The methods selected from the curve estimation and the best fit distributions obtained from the Arena simulation program are implemented and compared with the actual data. The comparison is performed for the five actual points. Figure 7a–c shows the actual data and the predicted data for the Salman Bay, Sharm Abhar and Jeddah Port areas,

respectively. The simulation results show an inverse tendency relative to the actual values, so it is excluded as a prediction method as shown in Fig. 7a, b. The simulation results are not realistic for these two areas because they are not available to be expanded, and they can be reduced. Moreover, the Jeddah Port area is expected to be expanded in the future; the simulation approach is better as shown in Fig. 7c.

4.2 Comparison of the Prediction Results of the Four Models

The summary of the future predictions for the three areas from 1972 to 2025 and Fig. 8a, b, and c show the prediction results as represented by Table 3. The inverse and logarithmic methods are proven to be better than the other methods for the Salman Bay area. Simulation (using a lognormal distribution) is excluded because its results are very far from the actual data, and it is clear in Fig. 8a that the MSE and MAD for the simulation method are also very high. For the Sharm Abhar

Table 3 Comparison of prediction method results for Salman Bay, Sharm Abhar and Jeddah Port

Criteria	Actual data			Prediction															
				Linear regression			Logarithmic			Inverse			Power			Simulation		
	Salman Bay	Sharm Abhar	Jeddah Port	Salman Bay	Sharm Abhar	Jeddah Port	Salman Bay	Sharm Abhar	Jeddah Port	Salman Bay	Sharm Abhar	Jeddah Port	Salman Bay	Sharm Abhar	Jeddah Port	Salman Bay	Sharm Abhar	Jeddah Port
Min	23.89	4.59	41.87	29.641	4.329	36.425	30.519	4.4232	35.692	30.595	4.4262	35.569	35.933	4.516	36.906	20.877	4.600	41.417
Max	42.64	6.42	58.98	30.277	6.078	53.120	31.195	6.1703	52.427	31.286	6.1738	52.323	35.957	6.168	51.595	65.941	7.654	68.569
Average	30.83	5.49	45.832	29.959	5.203	44.773	30.858	5.2930	44.023	30.943	5.2924	43.974	43.817 35.945	5.297	43.817	34.353	5.480	45.491
Mean square error (MSE)				43.120	0.164	22.408	42.230	0.8846	21.451	42.230	30.424	21.389	68.400	0.144	20.294	118.07	0.581	60.460
Mean absolute deviation (MAD)				0.944	0.089	0.862	0.0490	0.0002	0.1184	0.0340	0.0002	0.0270	5.110	0.006	0.311	0.135	0.017	3.574

Table 4 Average percent change in spatial borders using geometric mean

Year	Average percent change of spatial bordered area in km^2 over the years		
	Salman Bay (%)	Sharm Abhar (%)	Jeddah Port (%)
1972	–	–	–
1984	4.21	−0.66	−2.74
1990	−7.94	−1.46	0.54
2000	2.63	−1.52	−0.46
2016	−0.07	0.76	0.05

area and according to the MAD, the logarithmic, inverse and power methods are better than other methods, as shown in Table 3 and Fig. 8b. The Sharm Abhar area is not expected to be expanded in the future, so the simulation approach based on the Weibull distribution, being the best fit distribution, is excluded. For the Jeddah port area, a port that could expand in the future, we found that simulation approaches based on the lognormal distribution provide results that are better than for the other methods, as shown in Table 3 and Fig. 8c. The simulation-based gamma, beta, lognormal, Weibull and Erlang distribution results are compared, and the method with more realistic expected values is selected, which is lognormal.

For summary statistics, the geometric mean is calculated to find an average percent change over a period of time (Table 4). The rate of increase/decrease is determined by the following formula:

$$\text{G.M} = \sqrt[n]{\frac{\text{value at the end of period}}{\text{value at the start of period}}} - 1$$

Regarding the average percent change in the area, Table 4 shows a mix of increases and decreases. For Salman Bay, the largest decrease is witnessed from 1984 to 1990, which is almost 12%. However, a large increase of almost 10.50% is also witnessed in Salman Bay from 1990 to 2000. Sharm Abhar decreased up to 2000, but then it shows an increase of 0.76% in 2016. Jeddah Port, on the other hand, has intermittent increases and decreases, but the amount of decrease declined from −2.74% in 1984 to −0.46% in 2000.

5 Conclusions and Recommendations

We conclude our study with the following conclusions and recommendations.

(a) The changes occurring from 1972 to 2016 in the coastal borders of the study area resulted from the extensive establishment of random projects. The accreted processes of coastline areas were due to the effects of geo-environmental natural processes and anthropogenic activities.

(b) The efforts of the establishment of projects and filling processes along the Salman Bay area, Sharm Abhar and Jeddah Port caused shrinkage to and extension of the spatially bordering coastline.

(c) The study showed the significance of remote sensing applications and modern satellite imaging technology as operative tools in the study of sustainable progress.

(d) The findings of the current study can be used to establish a database for the study and rational management of the coastal areas in the future.

(e) A continuous monitoring program should be formulated for the study area to ensure continuous monitoring of the changes occurring in the area.

(f) Frequent assessments of geo-environmental impacts and ancillary geological studies must continue for the existing construction projects.

(g) Statistical techniques used for forecasting the areas can be employed by the decision makers and not only depend on the highest R^2 but also the incorporation of the least squares error; the decision maker can then select the suitable model for the forecast on the basis of the results.

(h) The simulation approach is a good approach for the prediction and simulation of real cases such as Jeddah Port.

(i) Prediction methods used in this study can be updated and merged with other techniques such as genetic algorithm (GA), particle swarm (PS) and ant colony (AC) tools. As a future implication, it is suggested that artificial neural networks (ANNs) may also be used to predict the study area.

References

1. Wukai, L.; Desheng, J.; Lijun, Y.; Jiajing, P.; Rui, Qu; Sun, Tao: Numerical simulation of temperature field and prediction of microstructure in friction hydro pillar processing. J. Mater. Process. Technol. **252**, 370–380 (2018)

2. Alesheikh, A.; Sadeghi, F.; Talebzade, A.: Improving classification accuracy using external knowledge. GIM Int. **17**(8), 12–15 (2003)

3. Abdullah, F.; Lalit, K.: Land use and land cover change detection in the Saudi Arabian desert cities of Makkah and Al-Taif using satellite data. Adv. Remote Sens. **3**, 106–119 (2014). https://doi.org/10.4236/ars.2014.33009

4. Anirban, M.; Sandip, M.; Samadrita, M.; Subhajit, G.; Sugata, H.; Debasish, M.: Automatic shoreline detection and future prediction: a case study on Puri Coast, Bay of Bengal, India. Eur. J. Remote Sens. **45**, 201–213 (2012). https://doi.org/10.5721/eujrs20124519

5. Mashael, Al Saud: Assessment of flood hazard of Jeddah Area 2009, Saudi Arabia. J. Water Resour. Protect. **2**, 839–847 (2010). https://doi.org/10.4236/jwarp.2010.29099

6. Amal, Al-Sheikh: Management of environmental degradation of Jeddah coastal zone, Saudi Arabia, using remote sensing and geographic information systems. J. Am. Sci. **7**, 665–673 (2011)

7. Moore, T.; AI-Rehaili, H.: Geologic map of the Makkah Quadrangle, sheet 21D, Kingdom of Saudi Arabia, Saudi Arabian Directorate General of Mineral Resources. Geoscience Map GM-107C, scale 1:250,000 (1989)

8. Kaufman, Y.; Wald, L.; Remer, B.; Gao, R.; Li, R.; Flynn, L.: The MODIS 2.1-mm channel—correlation with visible reflectance for use in remote sensing of aerosol. IEEE Trans. Geosci. Remote Sens. **35**, 1286–1298 (1997)

9. Matthew, M.; Golden, A.; Berk, S.; Richtsmeier, R.; Levine, L.; Bernstein, P.; Acharya, G.; Anderson, G.; Felde, M.; Hoke, A.; Ratkowski, H.; Burke, R.; Kaiser, D.; Miller, D.: Status of atmospheric correction using a MODTRAN4-based algorithm. In: SPIE Proceedings, Algorithms for Multispectral, Hyperspectral, and Ultraspectral Imagery VI, vol. 4049, pp. 199–207 (2000)

10. Van, T.; Binh, T.: Application of remote sensing for shoreline change detection in Cuu Long estuary. VNU J. Sci. Earth Sci. **25**, 217–227 (2009)

11. Claire, C.; Pham, V.; Pham, N.; Hoang, P.; Lam, N.: Remote sensing application for coastline detection in Ca Mau, Mekong delta. In: International Symposium on Geoinformatics for Spatial Infrastructure Development in Earth and Allied Sciences, pp. 1–6 (2012)

12. Aedla, R.; Dwarakish, G.; Reddy, V.: Automatic shoreline detection and change detection analysis of Netravati–Gurpur River mouth using histogram equalization and adaptive thresholding techniques. Aquat. Procedia **4**, 563–570 (2015)

13. Arismar, M.; Gonçalves, J.; Hélder, D.; Wallace, B.: Practical partial discharge pulse generation and location within transformer windings using regression models adjusted with simulated signals. Electr. Power Syst. Res. **157**, 118–125 (2016)

14. Hanke, J.; Wichern, D.: Business Forecasting 9th Edition. Pearson New International Edition (2014)

15. Vaidyanathan, P.: The Theory of Linear Prediction, Copyright © 2008 by Morgan and Claypool Publisher. Marcel and Göktuğ, 2018 (2008)

16. Bin, Z.; Jiemin, Z.; Mao, L.: Prediction of sinter yield and strength in iron ore sintering process by numerical simulation. Appl. Therm. Eng. **131**(25), 70–79 (2018)

17. Marcel, B.; Göktuğ, A.: Prediction of CO_2-induced plasticization pressure in polyimides via atomistic simulations. J. Membr. Sci. **547**, 146–155 (2018)

18. Tran, T.; Trinh, T.: Shoreline change detection to serve sustainable management of coastal zone in Cu Long Estuary. In: Proceedings of the International Symposium on Geoinformatics for Spatial Infrastructure Development in Earth and Allied Sciences.

Retrieved December 27, 2011 from http://wgrass.media.osaka-cu.ac.jp/gisideas08/viewpaper.php?id=247

19. Ayesha, S.; Charles, H.; Robert, A.; Neil, L.; John, J.: The predictive accuracy of shoreline change rate methods and alongshore beach variation on Maui, Hawaii. J. Coast. Res. **23**, 87–105 (2005). https://doi.org/10.2112/05-0521.1

20. Camila, M.; Nakata, O.; Léa, S.; Daniel, S.: This tool for heat island simulation: a GIS extension model to calculate urban heat island intensity based on urban geometry. Comput. Environ. Urban Syst. **67**, 157–168 (2018)

21. Fengli, Z.; Dana, J.; Mark, J.; David, W.; Robert, F.; Wangan, Jinjiang: Decision support system integrating GIS with simulation and optimization for a biofuel supply chain. Renew. Energy **85**, 740–748 (2016)

22. Sadik, K.; Amirreza, M.; Khaleghi, M.; Hamidi, Y.; Ferenc, S.; Guzin, B.; Young, S.: An Integrated GIS, optimization and simulation framework for optimal PV size and location in campus area environments. Appl. Energy **113**, 1601–1613 (2014)

23. Cowell, P.; Roy, P.; Jones, R.: Simulation of large-scale coastal change using a morphological behavior model. Mar. Geol. **126**, 45–61 (1995)

24. Alesheikh, A.; Blais, J.; Chapman, M.; Karimi, H.: Rigorous geospatial data uncertainty models for GIS in spatial accuracy assessment: land information uncertainty in natural resources, chapter 24. Ann Arbor Press, Michigan (1999)